Journal of Hydrology: Regional Studies 59 (2025) 102304

Contents lists available at ScienceDirect

Journal of Hydrology: Regional Studies

journal homepage: www.elsevier.com/locate/ejrh

Quantifying the impact of nuisance flooding on urban coastal communities under present and future climatic conditions: Norfolk, Virginia as a case study

Jiwoo Jeong [a,*], Sergio A. Barbosa [a,b,c], Jonathan L. Goodall [a]

[a] Department of Civil and Environmental Engineering, University of Virginia, Charlottesville, VA 22904, USA
[b] Environmental Institute, University of Virginia, Charlottesville, VA 22902, USA
[c] Now at Environmental Sciences Division, Oak Ridge National Laboratory, Oak Ridge, TN 37831, USA

ARTICLE INFO

Keywords:
Nuisance flooding
Compound flooding
Coastal communities
2D hydrodynamic modeling
Climate change

ABSTRACT

Study region: Norfolk, Virginia, United States
Study focus: Nuisance flooding, characterized by frequent but minor floods, has been on the rise and the trend is expected to continue due to climate change. Utilizing a two-dimensional surface flow / one-dimensional pipe hydrodynamic model, this study presents a methodology for simulating flooding from low return period tidal and rainfall events to quantify the impact of nuisance flooding on urban coastal communities under present and future climatic conditions. Applying the methodology, the results show the impact of nuisance flooding from tidal alone and compound (i.e., rainfall and tide) events.
New hydrologic insights for the region: Using 2020 as a base year, the model suggests tidal nuisance flooding (TNF) impacts approximately 4 % (1.87 km^2) of the study area. With a projected 1-meter sea-level rise by 2100, the TNF extent is projected to increase to approximately 12 % (5.85 km^2) — more than tripling the 2020 TNF extent. For the 2020 base year, when rainfall and high tide occur simultaneously, compound nuisance flooding (CNF) leads to 11 % (5.15 km^2) of the study area being inundated. By 2100, the projected inundated area by CNF is estimated to be 20 % (9.41 km^2). Overall, sea level rise drives the expansion of TNF along riverbanks and adjacent areas, while submerging many urban drainage system outlets. This prevents efficient rainfall drainage, which causes CNF on inland low-lying areas.

1. Introduction

Urbanization and climate change are two important factors in the increasing risk of urban flooding (Skougaard Kaspersen et al., 2017). Urbanization has led to an increase in impervious surfaces and a greater amount of direct runoff of rainwater from urban watersheds (Konrad, 2003; Leopold, 1968). Stormwater infrastructure systems for handling this runoff were designed assuming stationary rainfall and tidal conditions, and their adaptation to changing climate conditions presents a challenge for coastal communities living in urbanized areas (Chen et al., 2021). Climate change is altering rainfall frequency and intensity that have been assumed to be stationary (IPCC, 2021). As a result, many urban areas are at a higher risk of flooding because their existing stormwater infrastructure is inadequate for future climate conditions.

* Corresponding author.
E-mail address: neq7xb@virginia.edu (J. Jeong).

https://doi.org/10.1016/j.ejrh.2025.102304
Received 18 June 2024; Received in revised form 14 January 2025; Accepted 3 March 2025
Available online 13 March 2025
2214-5818/

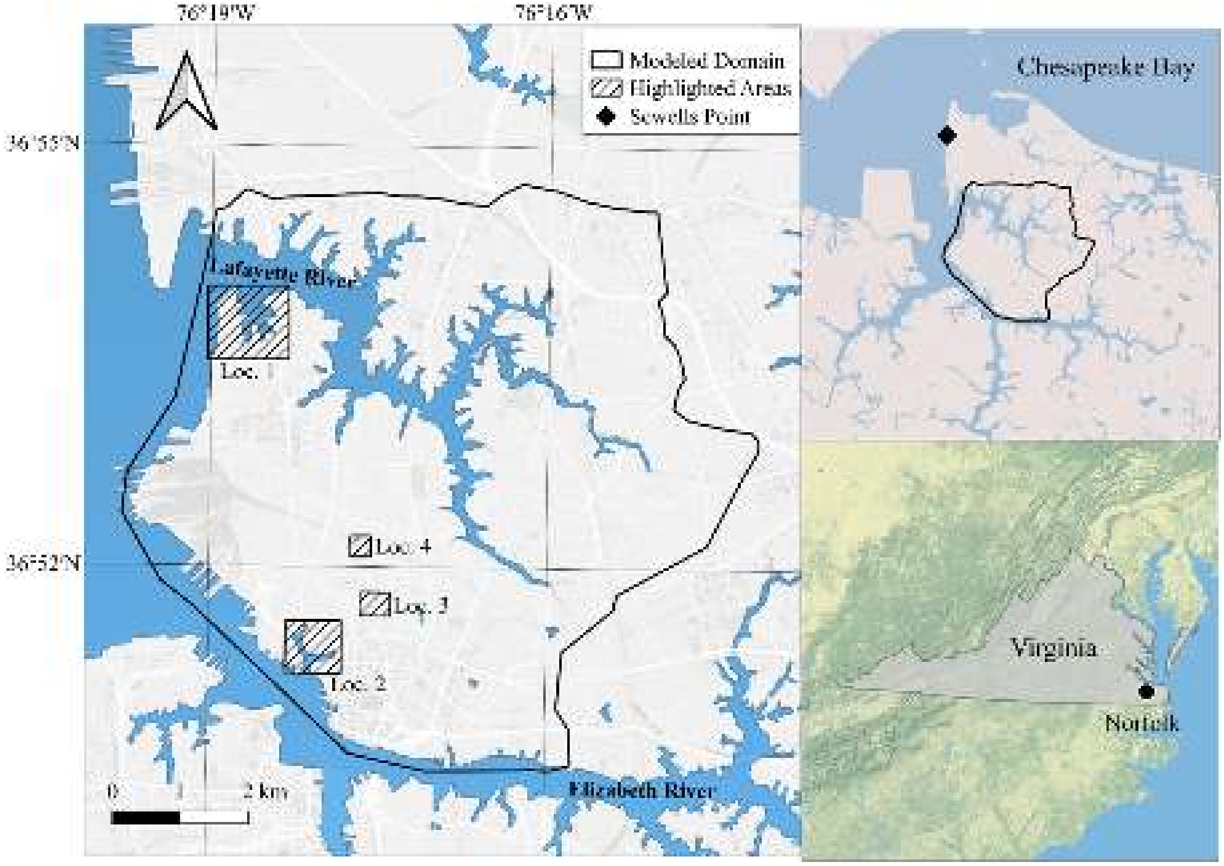

Fig. 1. Modeling domain in Norfolk, VA and the four locations highlighted in the Results and Discussion section.

Coastal regions are particularly vulnerable to an increased threat of flooding due to factors like rising sea levels and land subsidence (Devlin et al., 2017; Sweet et al., 2018). Coastal flooding can occur due to high tides, intense rainfall, or a combination of the two called compound flooding. Nuisance flooding describes flooding occurrences that happen more frequently and may impact only a portion of a community. Moftakhari et al. (2018) defined the concept of nuisance flooding as "low-level inundation" that does not pose significant threats to public safety or cause major property damage, regardless of the source. The frequency of nuisance flooding in the United States has increased dramatically over the past several decades (Karegar et al., 2017; Moftakhari et al., 2015; Sweet et al., 2014). Norfolk, Virginia, situated along the east coast of the United States, is a case study for an urban area experiencing increased nuisance flooding risk. Burgos et al. (2018) indicated that nuisance flooding in Norfolk has increased 325 % since 1960. Sweet et al. (2022) found that nuisance flooding in Norfolk has grown from about five days in 2000 to 10–15 days in 2020. Moreover, this number could reach 85–125 days by 2050. Ezer (2022) found that storm surge in Norfolk only reached 1.6 m once in the past 90 years but may exceed 1.6 m weekly or even daily by 2100 due to projected sea level rise.

While flood impact studies typically highlight extreme events, more studies are needed to understand the escalating impact of relatively frequent, small-magnitude nuisance events (e.g., annual or even monthly return periods) (Moftakhari et al., 2018). Nuisance flooding can disrupt routine day-to-day activities, strain infrastructure systems such as roadways and sewers, and cause minor property damage due to low water depths (Moftakhari et al., 2018). Moreover, certain regions will experience an accumulating asset exposure due to the repeated occurrence of these relatively small events over time (Moftakhari et al., 2017). Given the anticipated increase in both the frequency and scale of these nuisance floods due to climate change, the need for effective quantification of the impacts and creative countermeasures becomes apparent.

Furthermore, while previous studies have predominantly focused solely on the role of tides, storm surge, and sea-level rise on flooding (Camelo et al., 2020; Hino et al., 2019; Woodruff et al., 2013), it is important to also recognize the role of rainfall and compound events in nuisance flooding. Coastal floods are often caused by compound flooding (Hendry et al., 2019), and recent research has explored instances of compound floods using terms like joint impact (Lian et al., 2013), compound effect (Kew et al., 2013) and combined impact (Karamouz et al., 2015). Wahl et al. (2015) introduced the term compound flooding and presented evidence of a significant increase in simultaneous storm tide and heavy rainfall events across major U.S. coastal cities over the past century. Batten et al. (2017) demonstrated that over 50 % of rainfall events occurred when the sea water level was higher than the average daily high tide in the coastal region of Virginia. In urbanized coastal cities like Norfolk, it is evident that when compound flooding occurs, the flooded areas will expand. This is in large part due to high tide hampering the capacity of the stormwater drainage system to alleviate flooding by backing up seawater into these systems.

In order to effectively mitigate the impact of floods on humans and property, it is crucial to have an understanding of the flood extent and vulnerable areas to implement appropriate countermeasures (Lendering et al., 2016). Currently, research on nuisance flooding has primarily focused on predicting the degree of sea level rise and the frequency of flooding events, leaving the extent and depth of flooding uncertain. The National Oceanic and Atmospheric Administration (NOAA) has developed the "Sea Level Rise Viewer", which visually illustrates the impacted areas and the depth of coastal flooding due to rising sea levels. However, it does not account for the influence of rainfall and compound flooding. Achieving this analysis necessitates the use of hydraulic and hydrological models for simulation of complex urban drainage systems. Modeling urban regions poses several challenges due to their unique characteristics. Coastal regions are typically characterized by low-relief terrains, complicating water routing. Consequently, two-dimensional (2D) hydrodynamic models are more reliable for simulating urban floods in such conditions (Leandro et al., 2009). Nevertheless, 2D models alone are insufficient due to the critical role of underground pipe drainage systems in flood modeling within urban catchments. To realistically simulate flooding in urbanized coastal cities, flood models must be capable of simulating the dynamics of 2D surface flow, the one-dimensional (1D) pipe flow in the underground drainage system, and the interactions between the two systems. As a result, in this study we utilize a coupled model combining 2D overland and 1D pipe components (Bazin et al., 2014; Shen et al., 2019).

The primary contribution of this study is to provide a methodology for quantifying compound nuisance flooding vulnerability that can be repeated for other coastal urban communities. A secondary contribution is to demonstrate this methodology for assessing the impact of nuisance flooding in Norfolk. Building on prior research, this study advances and utilizes a 2D overland / 1D pipe hydrodynamic model described in Shen et al. (2022). Different scenarios are considered using that model: (1) tidal nuisance flooding (TNF) due to high tide without rainfall, (2) compound nuisance flooding (CNF) due to rainfall and high tide, and (3) climate change impacts to future TNF and CNF events. Through this process, we identify the portion of the study area impacted by nuisance flooding, and how the depth and extent of nuisance flooding increases as climate change affects rainfall intensity and sea level rise.

2. Materials and methods

2.1. Study area

Norfolk, Virginia is located on the southern shore of Chesapeake Bay on the east coast of the United States. The city is bounded on three sides by tidal waters, with tidally influenced tributaries reaching inland. The study area covered in this paper encompasses a portion of Norfolk and spans 56.4 km^2, including 8.7 km^2 of open water, as shown in Fig. 1. The four locations are highlighted in Fig. 1 because they exhibit noticeable changes as sea levels rise and rainfall intensity increases, as will be discussed in the Results and Discussion section. Location 1 refers to Edgewater Haven Bay, and Location 2 refers to the Hague. Both locations are susceptible to sea level rise due to their proximity to tidally influenced water bodies. Locations 3 and 4 are low-lying areas situated inland, near Debree and Llewellyn Avenues and Armistead Avenue, respectively.

The study area is bordered by the Elizabeth River to the south and west, with the Lafayette River running through the center and merging with the Elizabeth River toward the northwest. The Elizabeth River flows northward into the Chesapeake Bay, with Sewells Point located approximately 6 km north of their confluence. Tides at Sewells Point are semidiurnal, with two high and two low tides each day. The mean high water level is 0.287 m, and the mean low water level is −0.453 m according to the North American Vertical Datum of 1988 (NAVD88). While there is a slight time lag between river gauges and Sewells Point, the water levels of both rivers are influenced by these tides and exhibit the same cyclical tidal patterns.

Norfolk's vulnerability to flooding stems from several key factors. The rate of sea level rise along the mid-Atlantic coast of the United States, where Norfolk is situated, exceeds the global average (Kopp, 2013). With an average elevation of 3.14 m, Norfolk is prone to flooding from storm surge and high tides. Additionally, the city has a substantial impervious surface coverage, accounting for 41 % of the study area (The City of Norfolk, 2018), which increases the risk of rainfall-driven flooding. Climate change further exacerbates Norfolk's flood risk by increasing rainfall intensity (Morsy et al., 2019; Sridhar et al., 2019) and sea level rise. The Federal Emergency Management Agency (FEMA, 2016) reported that the Special Flood Hazard Area (SFHA) covers approximately 36 % of Norfolk (50.8 km^2 of the total 140.1 km^2). This represents a 7 % expansion (10.1 km^2) in SFHA from the previous flood insurance rate map done in 2010 and underscores the city's growing vulnerability to flooding.

2.2. Urban flood model

TUFLOW (Two-dimensional Unsteady FLOW) is a hydrodynamic model designed for simulating depth-averaged, one and two-dimensional free-surface flows. TUFLOW solves the full 2D depth averaged momentum and continuity equations for shallow water free surface flows and incorporates the full functionality of the ESTRY, its 1D hydraulic solver (Syme, 2001). TUFLOW was adopted for this study because it is capable of simulating both surface flow on a 2D domain and pipe flow via its 1D functionality along with a dynamic link between the two domains. Hunter et al. (2008) compared six 2D hydraulic models, including TUFLOW, to simulate surface flow in urban areas and found that all models produced plausible results. Zhang et al. (2016) developed a new three-dimensional (3D) model and simulated a flood event in Glasgow, comparing its performance with the simulation results of the six 2D hydraulic models from Hunter et al. (2008). The authors identified that the 3D modeling results generally matched TUFLOW better than the other 2D models investigated in their study.

In this study, flood simulations in Norfolk were conducted using the TUFLOW model described in Shen et al. (2022). It incorporates

Table 1
Parameters used for the hydrodynamic model.

Parameters	Type	Value
Manning's n value of 2D overland surface	Asphalt	0.012
	Concrete	0.013
	Other urban features	0.012
	Grassland	0.015
	Shrub land	0.4
Manning's n value of 1D pipes	Plastic pipe	0.012
	Concrete pipe	0.014
	Cast iron pipe	0.013
	Corrugated-metal pipe	0.015
	Brick	0.014

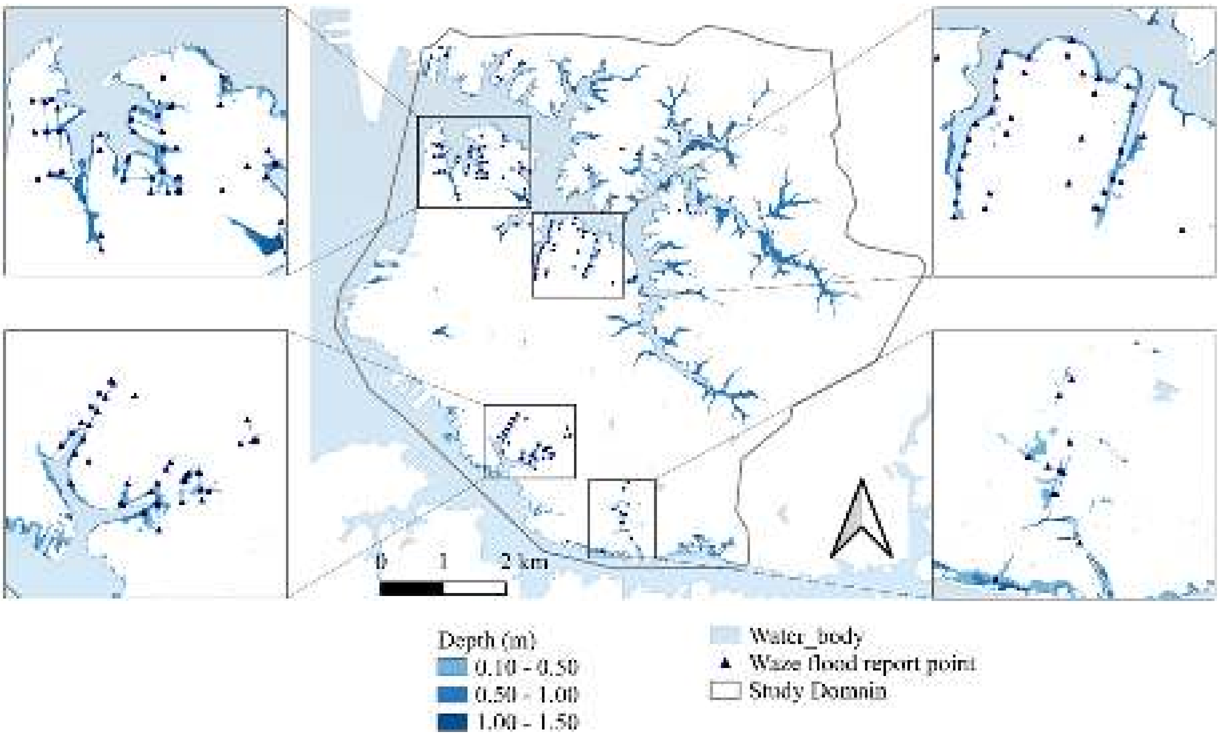

Fig. 2. Comparison of Waze flood reports and model simulation results for May 11, 2024.

the digital elevation model (DEM) and data on the stormwater drainage system within the study area. There are more than 29000 buildings and 9087 pipe sections with a total length of about 222 km in the model. Among them, small structures that did not meet standards were excluded to reduce the complexity of the model. For the parameter settings, Manning's roughness coefficients for overland flow were assigned to the 2D domain based on land cover types, as suggested by McCuen (1998). Similarly, different roughness coefficients were applied to various types of pipelines in the model. The specific Manning's coefficients used in this study are listed in Table 1. Norfolk has a relatively low average ground elevation of 3.1 m. The study area also has an average imperviousness ratio of 41 % and a shallow groundwater level that can rise to the surface during storm events. While infiltration can influence certain flooding scenarios, this study adopts saturated conditions to represent the worst-case scenario. Previous studies, such as Shen et al. (2022), support the assumption of saturated conditions in coastal urban flooding. Accordingly, the model assumes that non-impervious surfaces are fully saturated at the start of the simulation.

To evaluate the urban flood model, Shen et al. (2022) used data from a USGS gauge in Norfolk's Hague Community, recorded during Hurricane Irene in 2011. The model closely matched USGS gauge water levels, slightly underestimating peak levels (by 0.02 m) and showing a minor phase shift (about 30 min). Given the limited availability of direct flood observations, they also incorporated drone footage captured by Norfolk's Emergency Management Department after Hurricane Matthew's peak on October 10, 2016, which proved particularly useful for flood extent analysis. Although the footage lacked key metadata for direct georeferencing, Shen et al. (2022) developed a method to identify flood edges by aligning them with local features (e.g., streetlamps and curbs) and generating contour lines from high-resolution LiDAR data to approximate the inundation boundary. By assuming a level water surface post-storm,

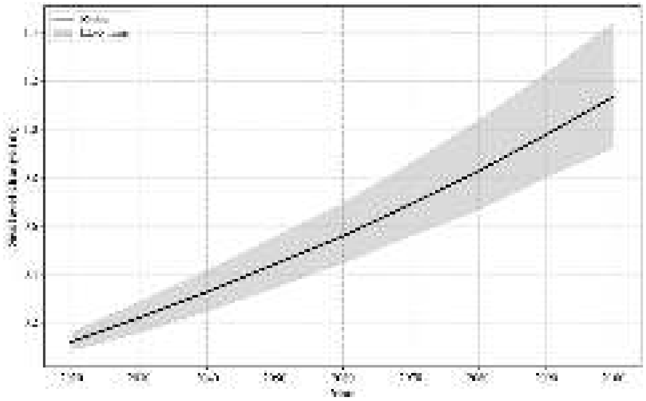

Fig. 3. The sea level changes under SSP5–8.5 scenario at Sewell Point.

this innovative approach enabled the extraction of flood extent across scenes within the study area. They compared these flooded areas with model simulation results, finding a 71–92 % match for each area, indicating the model's reliability.

In addition to the model evaluation by Shen et al. (2022), we conducted a reevaluation by testing the model against a recent flood event. Because the USGS station used by Shen et al. (2022) was not operational in recent years, we turned to crowdsourced flood reports to reevaluate the model. Prior research has shown how publicly contributed information, i.e. crowdsourced data such as images, videos, and reports shared on social media, can help fill data gaps and enhance model evaluation, particularly during flood events where on-the-ground measurements may be sparse (Fohringer et al., 2015; Helmrich et al., 2021). One valuable source of such data is the crowdsourced navigation app Waze (owned by Google), which collects a large volume of real-time road condition reports, including flood statuses from users. While concerns exist regarding the reliability of these reports due to the non-professional nature of the users (Helmrich et al., 2021), Praharaj et al. (2021) evaluated Waze's flood data and found it promising for road flood detection.

To assess model accuracy, we compared maximum inundation maps generated by the model with flood reports from the Waze platform. For the May 11, 2024 event, the highest tide level at Sewells Point reached approximately 1.2 m (NAVD88), and precipitation was minimal, indicating that the flooding was primarily caused by high tide. Within the study area, 200 flood incidents were reported on Waze. Fig. 2 illustrates the spatial distribution of the Waze flood reports (points) overlaid with the model's maximum inundation map (shaded areas). Waze flood reports were concentrated around the Lafayette and Elizabeth Rivers, with 176 of the 200 reports (88 %) aligning with flood locations predicted by the model within 10 m of the reported locations. The unmatched Waze reports were all located inland, primarily in the Park Place area. However, the ground elevation of the reported points in Park Place exceeded 1.5 m (NAVD88). Given the nature of Waze data, which relies on driver-reported information, these discrepancies do not suggest significant shortcomings in the model's performance.

2.3. Modeling scenarios

To align with the objective of studying impacts from nuisance flooding, a 1-year target return period was used for the modeling scenarios. The duration was selected as 1-hour to emphasize a shorter timeframe for nuisance flood events.

2.3.1. Tide events

NOAA established "nuisance level" for Norfolk at 0.53 m above mean higher high water (MHHW) (Sweet et al., 2014). This threshold has been applied in some studies, such as Burgos et al. (2018), Jacobs et al. (2018), and Sweet and Marra (2016), to identify instances of nuisance flooding. In this study, we also adopted this threshold as the present-day tidal boundary condition. The MHHW at Sewells Points is 0.35 m (NAVD88). Therefore, the nuisance tide elevation used in this study is 0.88 m (NAVD88).

Incorporating future tidal elevations as boundary conditions in urban flood prediction models requires anticipation of future relative sea level rise based on land subsidence and climate change scenarios. In this regard, the National Aeronautics and Space Administration (NASA) provides a valuable resource, the Sea Level Projection Tool (NASA, 2021). This tool enables users to visualize and download sea level projection data sourced from the IPCC 6th Assessment Report (AR6) and allows users to view both global and regional sea level projections from 2020 to 2150, along with variations depending on a future scenario or warming level (Fox-Kemper et al., 2021; Garner et al., 2021; Kopp et al., 2023).

Fig. 3 illustrates the sea level rise projections for the Sewells Point, focusing on the Shared Socioeconomic Pathways (SSP) 5–8.5 scenario. The thick solid line represents a median value, while shaded ranges depict the likely ranges. Median values are typically used as representative values. Therefore, in this study, the median values for each target year serve as future sea level rise values. The projections are the sum of the effects of six factors: glaciers, Greenland, Antarctica, land water storage, sterodynamic sea level, and vertical land movement.

The future target years in this study are 2050, 2070, and 2100, with projected sea level increases of 0.44 m, 0.69 m, and 1.13 m, respectively. It is assumed that the current nuisance level of 0.88 m reflects the expected sea level rise of 0.12 m in 2020. Therefore, an

Table 2
1-hour rainfall distribution extracted from a 24-hour rainfall distribution.

Time (hr)	Cumulative 24-hr rainfall ratio	Unadjusted cumulative 1-hr rainfall ratio	1-hr distribution time (hr)	Cumulative 1-hr rainfall ratio
11.5	0.2955	0.0000	0	0.0000
11.75	0.3516	0.0561	0.25	0.1371
12	0.4766	0.1250	0.5	0.4428
12.25	0.6484	0.1718	0.75	0.8629
12.5	0.7045	0.0561	1	1.0000

Table 3
Design rainfall distribution (mm) by target year.

Year	2020	2050 – 2100
15-min	4.5	5.3
30-min	10.1	11.9
45-min	13.9	16.4
60-min	4.5	5.3
Total	33.0	38.9

Table 4
The projected TNF area (km^2) for different flood inundation depths (d) around Edgewater Haven and Hague Community.

Location (Area)	Edgewater Haven (1.51)				Hague Community (1.75)			
Year	2020	2050	2070	2100	2020	2050	2070	2100
0.1 m < d ≤ 0.3 m	0.03	0.05	0.1	0.19	0.03	0.06	0.07	0.09
0.3 m < d ≤ 0.5 m	0.02	0.04	0.07	0.18	0.02	0.04	0.07	0.08
0.5 m < d	0.08	0.12	0.17	0.4	0.05	0.1	0.17	0.34
Total	0.13	0.21	0.34	0.77	0.1	0.2	0.31	0.51
	8.6 %	13.9 %	22.5 %	51.0 %	5.7 %	11.4 %	17.7 %	29.1 %

additional 0.32 m is added to 0.88 m to calculate the projected nuisance level for 2050, resulting in a level of 1.20 m. The nuisance levels for 2070 and 2100 are calculated in the same manner. As a result, the nuisance levels reflecting sea level changes under the SSP5–8.5 scenario are 0.88 m (2020), 1.20 m (2050), 1.45 m (2070), and 1.89 m (2100).

2.3.2. Compound events

We utilized the projected intensity-duration-frequency (IDF) curves for the Chesapeake Bay watershed and Virginia under the Representative Concentration Pathway (RCP) 4.5 and 8.5 scenarios by Miro et al. (2021) to estimate future rainfall events. The impact of climate change on hydrologic events is highly regional (Zhu et al., 2012; Kundzewicz et al., 2014) and assessments for updating IDF curves should be relevant to the specific project location (Morsy et al., 2019). Despite the introduction of the SSP scenario in the IPCC's 6th report in 2021, downscaled datasets based on the Coupled Model Intercomparison Project Phase (CMIP) 6 are not yet available. As a result, it is not feasible to develop precipitation change factors — representing the rate of increase in the IDF curve between historic and future periods —based on this new generation of global climate simulations (Miro et al., 2021). Miro et al. (2021) also conducted a comparison of global climate model-scale rainfall extremes between comparable CMIP5 and CMIP6 models and simulations. The authors found similar results for Virginia.

Miro et al. (2021) computed change factors for each return period and grid cell, aggregating these factors to the county scale. However, the authors did not explicitly project rainfall depth for a 1-year return period. The change factors indicated for return periods of 10 years or less uniformly stand at 1.18. Consequently, this consistent factor was applied to a 1-year return period. Considering that the 1-year Atlas 14 depth at the same location is recorded as 35.6 mm, applying the change factor yields a projected 1-year depth of 42.0 mm. In this study, compound flooding was simulated by using Atlas 14 rainfall depth data for the year 2020 (35.6 mm) and the projected depth (42.0 mm) within the time span from 2050 to 2100, as representative of rainfall for the years 2050, 2070, and 2100.

The precipitation estimates provided by Miro et al. (2021) are point estimates, and applying these values uniformly across the entire area may result in an overestimation of floods. Typically, precipitation depth decreases as the area increases. Therefore, when applying point precipitation uniformly, it must be converted into an area-average value (Kim et al., 2019). This conversion is achieved through the concept known as the areal reduction factor (ARF). In the United States, the commonly used ARF is based on Technical Report 29 (TP-29), proposed by the U.S. Weather Bureau in 1957. While there have been attempts to estimate ARF using new analytical methods, Svensson and Jones (2010) found that these methods have limitations, and traditional empirical ARF estimation methods still have strengths. Allen and DeGaetano (2005) and Kao et al. (2020) concluded that, for the United States, ARF estimations from TP-29 remain valid for watershed areas smaller than 1000 km^2. In addition, Pavlovic et al. (2016) derived ARFs using various methods, including scaling based on the same dataset, and compared the results. For a watershed area of 50 km^2, similar to the study area, each

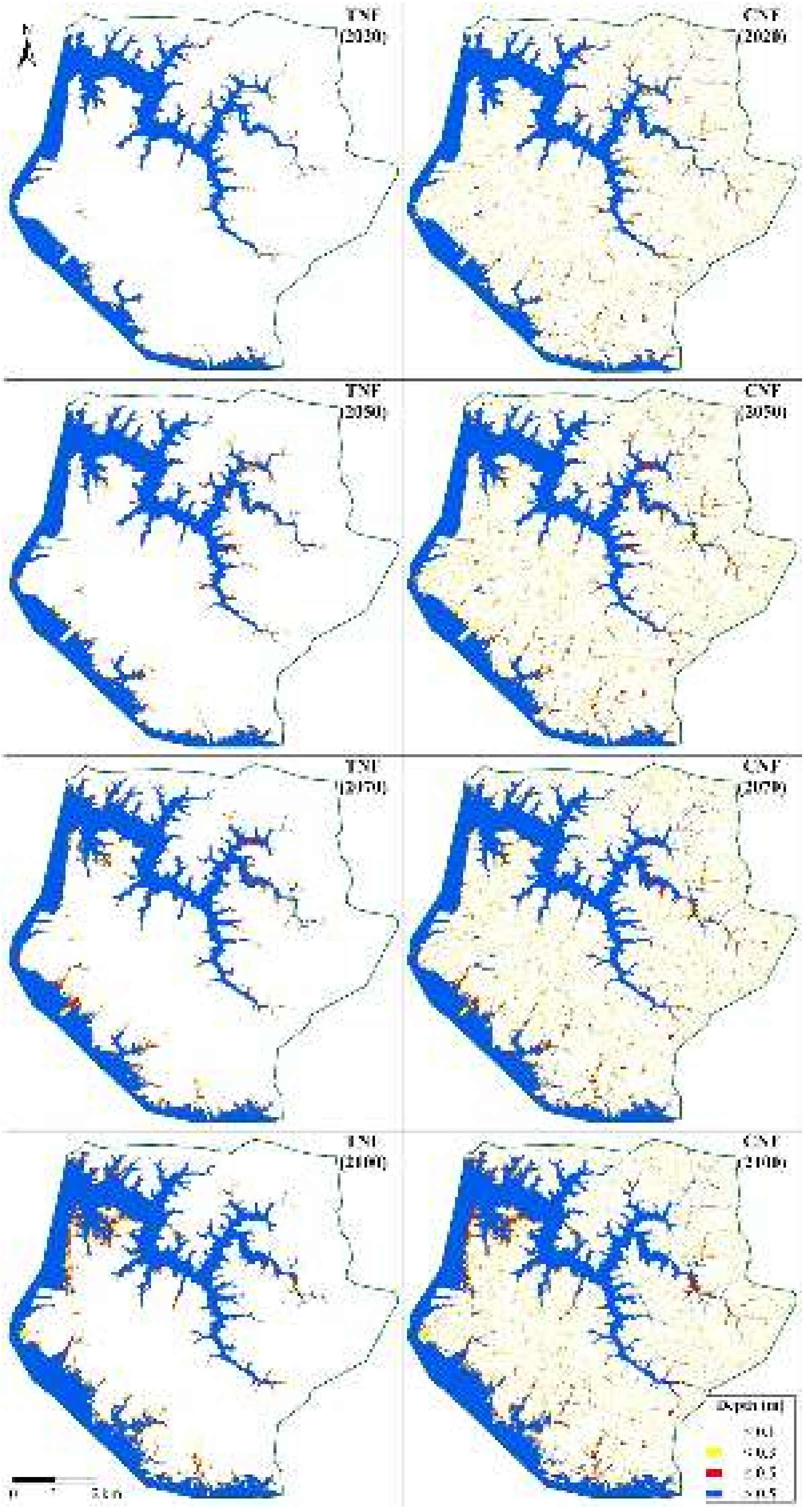

Fig. 4. Flooding maps by TNF (left), CNF (right) for the years 2020, 2050, 2070, and 2100, respectively.

method produced ARFs above 0.9, indicating comparable results across different methods. Therefore, we determined that using the traditional ARF estimation based on TP-29 is appropriate for such a small and homogenous area. Eagleson (1972) summarized the ARFs presented in TP-29:

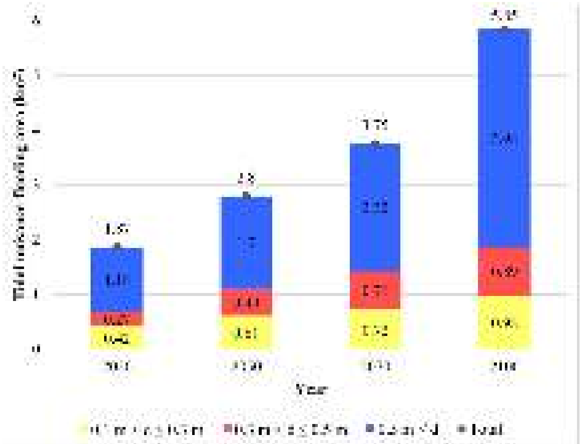

Fig. 5. The tidal nuisance flooding area (km^2) for different flood inundation depths (d) for the years 2020, 2050, 2070 and 2100.

$$ARF = 1 - \exp\left(-1.1t_d^{0.25}\right) + \exp\left(-1.1t_d^{0.25} - 0.01A\right) \quad (1)$$

where, t_d is the duration (hours) and A is the area (mi^2). The ARF curve presented in this report provides ARF values based on changes in area and duration. Since the study area is 21.8 mi^2, the ARF value provided is 0.93 for a 1-hour duration. Consequently, the projected rainfall, based on this ARF, is estimated at 33.0 mm for the year 2020 and 38.9 mm for the period spanning 2050–2100.

The study area is in the region of NOAA Type-C rainfall distribution zone, according to Merkel et al. (2015). However, it is important to note that the NOAA Type-C rainfall distribution is designed for a 24-hour duration. When distributing rainfall for shorter durations, such as 1 hour, it is not appropriate to use a distribution curve intended for much longer durations. Therefore, in this study, a different approach was adopted. NRCS (2019) provides a methodology for extracting rainfall distributions for shorter durations from the standard 24-hour rainfall distribution. NOAA Type-C 24-hour rainfall distribution table at a 0.1-hour interval is available through WinTR-20 software (NRCS, 2022). The duration should be centered on 12 hours, so the 1-hour period will start at 11.5 hours and end at 12.5 hours. Interpolation is applied to determine ratios at 11.75 and 12.25 hours due to the interval of 0.1 hours. For a detailed illustration of this process, refer to Table 2. Table 3 presents the rainfall events by applying the respective rainfall intensities for each target year to the 1-hour rainfall distribution outlined in Table 2.

2.3.3. *Quantifying the extent of nuisance flooding*

This study classifies nuisance flood stages as follows: Stage 1 (10–30 cm), Stage 2 (30–50 cm), and Stage 3 (over 50 cm). Several studies contributed to defining these thresholds. Caradot et al. (2011) identified depths surpassing 30 cm as a serious level, while Yin et al. (2016) also highlighted that 30 cm matches the height of the air inlets for many vehicles. Fant et al. (2021) noted that a 13-cm water depth reaches the undercarriage of most vehicles. Silverman et al. (2022) considered 4 in. (approximately 14 cm) as the threshold for nuisance flooding, as it is expected to limit the mobility of cars. Jacobs et al. (2018) defined nuisance flooding as depths ranging from 30 to 60 cm. Lee et al. (2018) suggested the marginal flooding depths that impede human movement (20 cm for children, 50 cm for women, 70 cm for men) and the behavioral limit of 30 cm. Based on available information, depths below 10 cm generally pose minimal concern since most vehicles can still pass. However, when depths exceed 10 cm, low-height vehicles may face difficulties. If the depth exceeds 30 cm, regular vehicles, excluding specialized ones like trucks, cannot pass the road. This flood depth can also impact pedestrian movement. A water depth exceeding 50 cm indicates that both vehicles and pedestrians will be unable to pass. As a result, this study established water depth thresholds.

3. Results and discussion

Fig. 4 presents the simulation results for TNF (left) and CNF (right) for the years 2020, 2050, 2070, and 2100, displayed from top to bottom. TNF primarily occurs near tidal rivers and, as sea levels rise, the flooded area expands. However, by the year 2100, TNF continues to have minimal impact on inland areas. When comparing the simulation results between TNF and CNF of the same target year, it is evident that CNF results in flooding in inland areas as well, leading to a significant expansion of the overall flood areas. This highlights how Norfolk's stormwater drainage system can contribute to inland flooding during high tide conditions.

3.1. *Tidal nuisance flooding*

Fig. 5 provides the inundated area for TNF for the years 2020, 2050, 2070, and 2100. The projected extent of TNF, with an initial coverage of 1.87 km^2 at a tide level of 0.88 m in 2020, is expected to expand significantly. By 2100, with the tide level expected to reach 1.89 m, this extent is projected to increase to 5.85 km^2, a 3.1-fold increase. Notably, areas experiencing flood depths of 0.3 m or

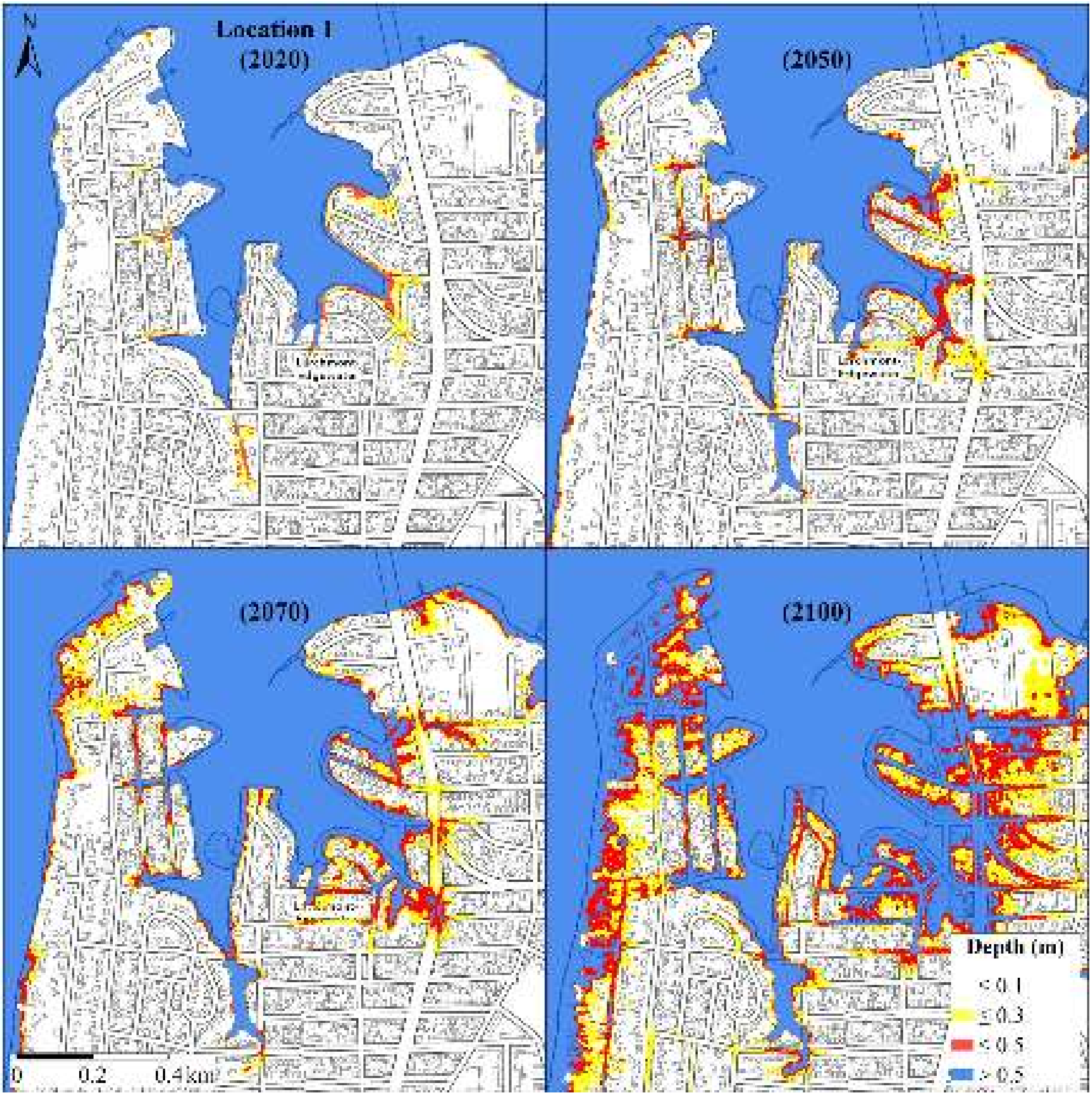

Fig. 6. Change in TNF area and depth at Edgewater Haven (location 1) for the years 2020, 2050, 2070 and 2100.

more comprise approximately 80 % of the flooding area, growing from 1.45 km^2 to 4.87 km^2, a 3.4-fold increase. This trend underscores the future impact caused by rising sea levels in the study region.

Figs. 6 and 7 illustrate the magnified views of TNF at Edgewater Haven on the Lafayette River (location 1) and at Hague on the Elizabeth River (location 2), respectively. These two areas, which are shown in Fig. 1, exhibit a more rapid escalation in both the extent and depth of TNF occurrences compared to the rest of the study area as sea levels rise, signifying their heightened vulnerability to inundation.

The land area of Edgewater Haven, depicted in Fig. 6, is approximately 1.51 km^2. It can be observed from Fig. 6 that this region is highly vulnerable to sea level rise, particularly the right side of the region being severely affected. The vulnerability can also be quantified numerically. In 2020, the expected area of TNF in this region is 0.13 km^2, accounting for about 8.7 % of the total area. TNF intensifies as sea levels rise and flooding area extends to 0.77 km^2, marking a 5.9-fold increase, which represents about 51 % of the region by 2100.

Location 2 depicted in Fig. 7 is the Hague neighborhood, with a land area of about 1.75 km^2. The expected area of TNF in this region in 2020 is 0.1 km^2, accounting for 5.7 % of the total area. With rising sea levels, TNF also increases and it covers 0.51 km^2, marking a 5.1-fold increase, representing about 29.1 % of the region by 2100. In addition, Fig. 7 highlights a crucial observation about the TNF

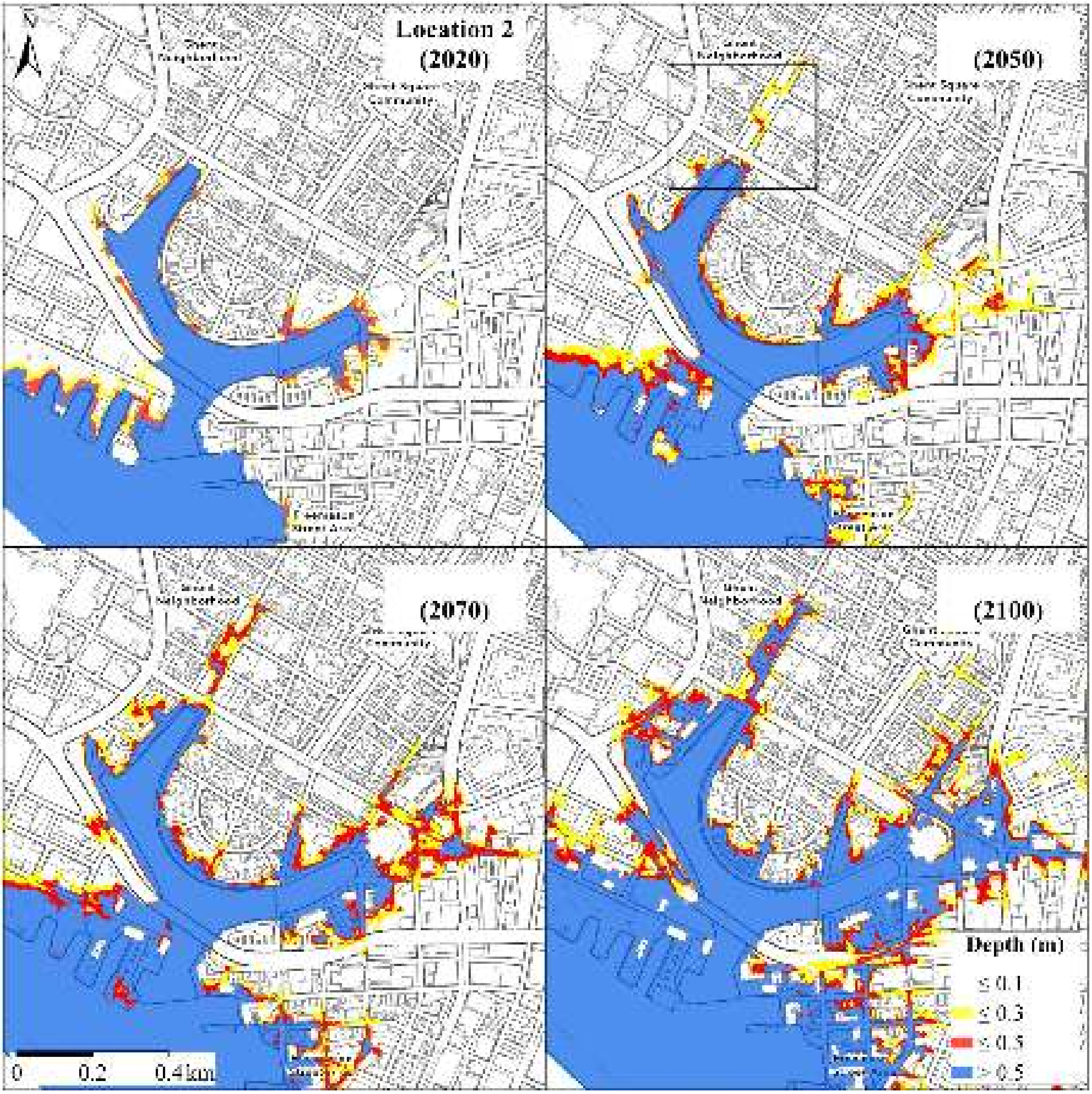

Fig. 7. Change in TNF area and depth at the Hague (location 2) for years 2020, 2050, 2070 and 2100.

pattern. The Stockley Gardens area, delineated by a box in Fig. 7, seems to lack a hydrological connection to nearby water bodies, attributed to the presence of the higher-elevated road (West Olney Rd.) separating them and preventing overland tidal flooding. In these simulations, assuming no rainfall, flooding in localized low-lying areas appears to result from backward pipe flow within the stormwater pipelines, due to the absence of tide gates or flap gates in the study area (Shen et al., 2022).

3.2. Compound nuisance flooding

Fig. 8 provides information on projected CNF areas based on tide and rainfall scenarios for the years 2020, 2050, 2070, and 2100. The projected extent of CNF, which initially covers 5.15 km^2 at a tide level of 0.88 m and rainfall of 33 mm in 2020, is expected to undergo significant increase. By 2100, with projected tide level and rainfall reaching 1.89 m and 39 mm respectively, this extent is expected to expand to 9.41 km^2, representing 20.0 % of the study area. When rainfall and high tide occur simultaneously, areas inundated by nuisance flooding experience a substantial increase. Compared to TNF, CNF exhibits a 3.28–3.94 km^2 increase in flooded area, with over 73 % of the augmented region experiencing inundation depth 0.1 m to 0.3 m. These results lead to the conclusion that effective rainwater drainage from the city becomes hindered during periods of high tide combined with rainfall, resulting in an

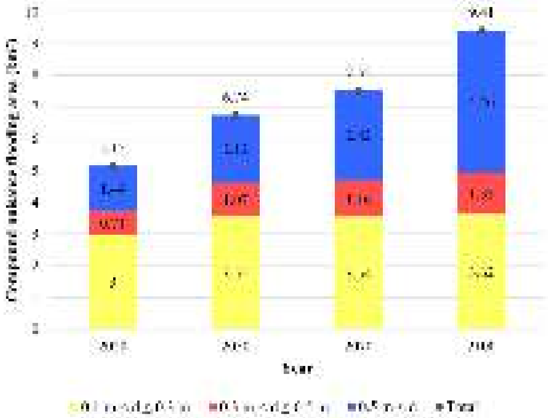

Fig. 8. The compound nuisance flooding area (km^2) for different water depths (d) for the years 2020, 2050, 2070 and 2100.

amplified extent and depth of flood occurrences.

When comparing TNF simulation results with DEM, it can be seen that inundated areas of inland region are mainly comprised of lowlands with an elevation of less than 3 m. Flooding with an inundation depth of 0.3 m or more on the road can hinder traffic of vehicles and people, and areas exceeding 0.3 m in depth are projected to expand from 2.15 km^2 in 2020 to 5.79 km^2 by 2100. Such roads can be found throughout inland region, making safe passage of vehicles and people challenging.

To study the progression of flooding with increasing rainfall, specific areas in the inland region were selected, spanning from Debree Avenue to Llewellyn Avenue on Park Place (location 3), and Armistead Avenue around Elmwood Cemetery (location 4). Even if the tide level remains below their ground elevations, nuisance flooding occurs when a 1-year return period rainfall is added. Fig. 9 shows the change in the occurrence pattern of nuisance flooding for locations 3 and 4, respectively. In this figure, the TNF range and inundation depth exhibit an increase in 2020 compared to TNF, attributed to amplified rainfall. However, from 2050 to 2100, where rainfall remains constant, the TNF range and depth demonstrate minimal variation.

The widespread flooding that occurs when high tide and rainfall coincide is related to the reduction in drainage capacity caused by high tide. During such compound events, pipe outlets may become partially or fully submerged. In this model, there are 407 outlets releasing stormwater into the Elizabeth and Lafayette Rivers. These outlets are categorized according to their submerged status at tide levels for each target year, as shown in Table 5. In the year 2020, only 56 outlets (14 %) remain unsubmerged, while 276 outlets (68 %) are fully submerged, and an additional 75 outlets partially submerged. In total, 351 outlets (86 %) are affected by tide. This highlights the severity of drainage capacity reduction due to the current tide level rise in Norfolk, a problem that will be exacerbated by further sea level rises. By the year 2100, only 10 outlets (2 %) are projected to remain unsubmerged. Excluding these, 397 outlets (98 %) will be submerged, with 364 outlets (89 %) fully submerged. In a submerged state, available hydraulic grade is minimal, and pipe networks convey a reduced flow (Shen et al., 2019; Taylor et al., 2015). In conclusion, as sea levels rise, Norfolk's stormwater infrastructure becomes increasingly inundated, leading to a diminished drainage capacity.

3.3. Discussion

Compared to previous studies, this research stands out in two key aspects. Firstly, it focused on a low return period rather than an extreme level. Secondly, unlike conducting individual flood simulations for each tide or rainfall event, this study undertook a flood simulation that combined both elements. The model used a foundational setup, including 'nuisance level' tide and 1-hour rainfall based on a 1-year return period. Moreover, to address the projected impacts of climate change, including rising sea levels and heightened rainfall intensity, additional scenarios were developed using the SSP5–8.5 and RCP8.5, representing the most conservative flooding projections.

3.3.1. Transferability of the methodology

The methodology applied in this study, utilizing a 2D surface/1D pipe hydrodynamic model, serves as a framework for evaluating the susceptibility of Norfolk to nuisance flooding. Extending this methodology to new areas, such as other coastal cities facing similar vulnerabilities, demands attention to specific prerequisites and considerations. Access to datasets, including DEMs and underground stormwater drainage systems, forms the foundation for constructing the model. Validating and calibrating the model relies heavily on actual flood measurement data, often a challenge in urban settings. Nevertheless, advancements in sensing capabilities present promising opportunities. For example, leveraging drone or surveillance camera data, social media reports, and vehicle driving records can help collect flood data and refine flood models (Shen et al., 2022; Wang et al., 2024). Incorporating sensors and deep learning technology can further enhance real-time flood simulation and prediction, which is crucial for mitigating flood damage.

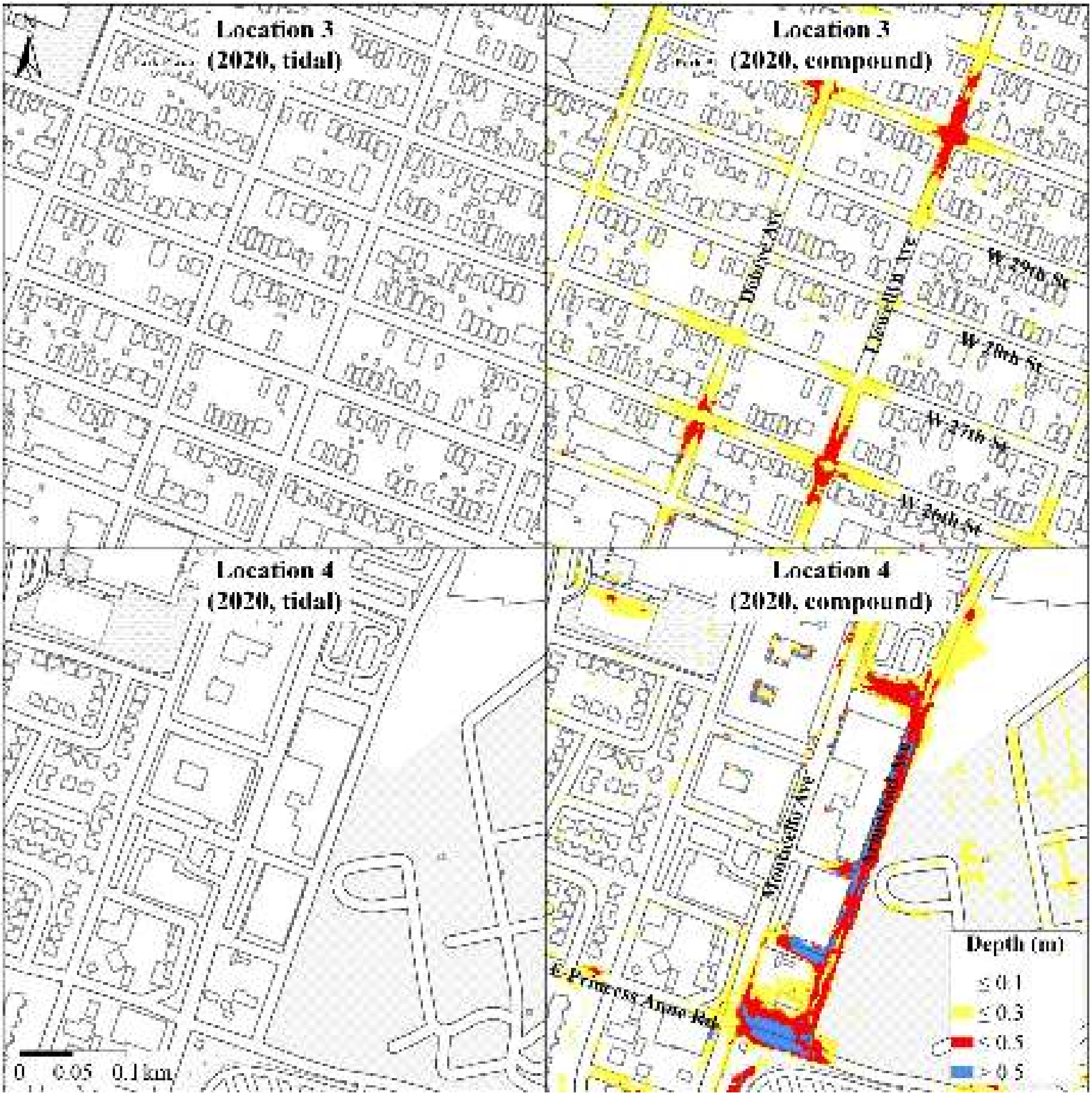

Fig. 9. Change of flood area and depth between tidal and compound nuisance flooding at Debree and Llewellyn Avenue (location 3), Armistead Avenue (location 4) for the year 2020.

Table 5
The status of outlets classified by tide levels in study area across the target years.

Year	2020	2050	2070	2100
Sea level (m)	**0.88**	**1.20**	**1.45**	**1.89**
Not submerged	56	32	23	10
Submerged (0–50 %)	35	28	16	11
Submerged (50–99 %)	40	37	36	22
Fully submerged	276	310	332	364

3.3.2. Assumptions and limitations of the study

Central to this study are key assumptions around projected sea level rise and rainfall patterns. The inherent uncertainties in climate change predictions and data availability affect the precision of model forecasts. To address these uncertainties, ongoing validation with real flood events is essential, as well as the incorporation of a wider range of flood scenarios based on varying sea level rise projections and rainfall intensities. This will allow for a more accurate assessment of the model's applicability across different environmental conditions. Additionally, we assumed no changes in the infrastructure in Norfolk; however, the city is advancing the coastal storm risk management project. As part of this project, barriers are planned to be constructed along the Elizabeth River shoreline and at the mouth of the Lafayette River. It is anticipated that upon completion of this project, there will be a mitigating effect on TNF occurring adjacent to these two rivers. Lastly, infiltration in urban flood modeling can affect simulation results, especially at relatively low rainfall intensities (Barbosa et al., 2025; Ryan et al., 2022). However, we assumed saturation of the pervious surface for conservative flood assessment, given the hydrological properties of coastal cities.

3.3.3. Opportunities for future research

Future research endeavors should concentrate on several focal points to advance this methodology. Firstly, the collection of additional flood measurement data remains pivotal, directly influencing model accuracy. Secondly, integrating novel data sources and analysis methods, such as machine learning algorithms and crowdsourced information, can enhance model calibration and flood forecasting capabilities. Moreover, ongoing research should prioritize broadening the methodology to encompass a wider array of scenarios, including changes in storm intensities, land use variations, infiltration variations, and infrastructure modifications. This expanded scope will increase the model's adaptability to evolving climate patterns and urban environments.

4. Conclusion

This study presents a methodology for quantifying the impact of nuisance flooding, demonstrating its application to assess the vulnerability of nuisance flooding in Norfolk. Building upon previous studies, we view nuisance flooding not solely as high-tide flooding but as frequent yet minor flooding regardless of its source. In addition to TNF, we simulated concurrent occurrences of high tide and rainfall (CNF) using a 2D surface/1D pipe flow integration model. TUFLOW effectively represented the study area's topography and extensive stormwater drainage system. The key findings of the simulation results are as follows.

(1) For TNF, the simulation results exhibit a consistent upward trend in the inundated areas as sea levels rise, primarily concentrated around the Lafayette and Elizabeth Rivers. With a projected 1-meter sea level increase by 2100, the TNF area is anticipated to reach 5.85 km^2, compared to the 1.87 km^2 observed in 2020, a 3.1-fold increase. However, inland areas are not significantly impacted by TNF.

(2) The CNF area, which measured 5.15 km^2 in 2020, is projected to increase to 9.41 km^2 by 2100, covering 20.0 % of the study area. This represents an increase ranging from 3.28 km^2 to 3.94 km^2 in flooded area compared to TNF. In addition, areas with inundation depths exceeding 0.3 m are projected to expand from 2.15 km^2 in 2020–5.79 km^2 by 2100. Inland lowlands with elevations below 3 m are likely to experience road inundation of 0.3 m or more, hindering vehicular and pedestrian traffic.

(3) Structural issues in Norfolk's stormwater drainage system impact both TNF and CNF. Currently, 86 % of the stormwater outlets in the study area are affected by the present 'nuisance level,' with 68 % fully submerged and 18 % partially submerged at this level. When sea level rises 1 m by 2100, this percentage is expected to increase to about 98 %, with 89 % fully submerged and 9 % partially submerged during nusiance events. The inundation of outlets poses a challenge to the system. Backward flow within the stormwater pipes causes flooding in localized low-lying areas, and simultaneously reduces the available hydraulic grade, resulting in diminished drainage through the system.

The key assumption of this study lies in setting tidal and rainfall conditions considering climate change, which is inherently uncertain. In this respect, uncertainties of future climatic conditions can be seen as limitations of this research. However, the concensus is that sea level rise and increased rainfall intensity will persist in the future for the study region. Therefore, this research has an advantage in being able to identify areas currently vulnerable to nuisance flooding and those expected to become vulnerable.

The methodology employed in this study serves as a framework for assessing Norfolk's vulnerability to nuisance flooding. Extending this methodology to other regions, such as coastal cities facing similar challenges, requires access to datasets, including DEMs and information on underground stormwater drainage systems.

CRediT authorship contribution statement

Barbosa Sergio A.: Writing – review & editing, Visualization, Supervision, Formal analysis. **Jeong Jiwoo:** Writing – review & editing, Writing – original draft, Visualization, Validation, Software, Resources, Project administration, Methodology, Investigation, Formal analysis, Data curation, Conceptualization. **Goodall Jonathan L.:** Writing – review & editing, Supervision, Project administration, Methodology, Funding acquisition, Conceptualization.

Declaration of Competing Interest

The authors declare that they have no known competing financial interests or personal relationships that could have appeared to influence the work reported in this paper.

Acknowledgements

This work was supported by the United States National Science Foundation (grant number 2209139) and the University of Virginia

Environmental Institute. We thank the multiple agencies that have supported the development of the sea-level rise projections and have made them publically available, and specifically the NASA Sea-Level Change Team for developing and hosting the IPCC AR6 Sea-Level Projection Tool.

Data availability

Data will be made available on request.

References

Allen, R.J., DeGaetano, A.T., 2005. Areal Reduction Factors for Two Eastern United States Regions with High Rain-Gauge Density. J. Hydrol. Eng. 10, 327–335. https://doi.org/10.1061/(ASCE)1084-0699(2005)10:4(327).

Barbosa, S.A., Wang, Y., Goodall, J.L., 2025. Exploring Infiltration Effects on Coastal Urban Flooding: Insights from Nuisance to Extreme Events Using 2D Hydrodynamic Modeling and Crowdsourced Flood Reports. Sci. Total Environ. 968, 178908. https://doi.org/10.1016/j.scitotenv.2025.178908.

Batten, B., Rosenberg, S., Sreetharan, M., 2017. Joint Occurrence and Probabilities of Tides and Rainfall. City of Virginia Beach. Available from: ⟨https://s3.us-east-1.amazonaws.com/virginia-beach-departments-docs/pw/Stormwater-Planning/Joint-Occurrence-and-Probablities-of-Tides-and-Rainfall-October-2017.pdf⟩ [Accessed June 7th, 2024].

Bazin, P.-H., Nakagawa, H., Kawaike, K., Paquier, A., Mignot, E., 2014. Modeling Flow Exchanges between a Street and an Underground Drainage Pipe during Urban Floods. J. Hydraul. Eng. 140, 04014051. https://doi.org/10.1061/(ASCE)HY.1943-7900.0000917.

Burgos, A.G., Hamlington, B.D., Thompson, P.R., Ray, R.D., 2018. Future Nuisance Flooding in Norfolk, VA, From Astronomical Tides and Annual to Decadal Internal Climate Variability. Geophys. Res. Lett. 45. https://doi.org/10.1029/2018GL079572.

Camelo, J., Mayo, T.L., Gutmann, E.D., 2020. Projected Climate Change Impacts on Hurricane Storm Surge Inundation in the Coastal United States. Front. Built Environ. 6, 588049. https://doi.org/10.3389/fbuil.2020.588049.

Caradot, N., Granger, D., Chapgier, J., Cherqui, F., Chocat, B., 2011. Urban flood risk assessment using sewer flooding databases. Water Sci. Technol. 64, 832–840. https://doi.org/10.2166/wst.2011.611.

Chen, W., Wang, W., Huang, G., Wang, Z., Lai, C., Yang, Z., 2021. The capacity of grey infrastructure in urban flood management: A comprehensive analysis of grey infrastructure and the green-grey approach. Int. J. Disaster Risk Reduct. 54, 102045. https://doi.org/10.1016/j.ijdrr.2021.102045.

Devlin, A.T., Jay, D.A., Talke, S.A., Zaron, E.D., Pan, J., Lin, H., 2017. Coupling of sea level and tidal range changes, with implications for future water levels. Sci. Rep. 7, 17021. https://doi.org/10.1038/s41598-017-17056-z.

Eagleson, P.S., 1972. Dynamics of flood frequency. Water Resour. Res. 8, 878–898. https://doi.org/10.1029/WR008i004p00878.

Ezer, T., 2022. A Demonstration of a Simple Methodology of Flood Prediction for a Coastal City Under Threat of Sea Level Rise: The Case of Norfolk, VA, USA. Earth'S. Future 10, e2022EF002786. https://doi.org/10.1029/2022EF002786.

Fant, C., Jacobs, J.M., Chinowsky, P., Sweet, W., Weiss, N., Sias, J.E., Martinich, J., Neumann, J.E., 2021. Mere Nuisance or Growing Threat? The Physical and Economic Impact of High Tide Flooding on US Road Networks. J. Infrastruct. Syst. 27, 04021044. https://doi.org/10.1061/(ASCE)IS.1943-555X.0000652.

FEMA, 2016. Flood Risk Report, City of Norfolk, Virginia Coastal Study. Available from: ⟨https://map1.msc.fema.gov/data/FRP/FRR_510104_Coastal_20160708.pdf?LOC=d708acf3264540688ded0ffca6622e95⟩ [Accessed June 7th, 2024].

Fohringer, J., Dransch, D., Kreibich, H., Schröter, K., 2015. Social media as an information source for rapid flood inundation mapping. Nat. Hazards Earth Syst. Sci. 15, 2725–2738. https://doi.org/10.5194/nhess-15-2725-2015.

Fox-Kemper, B., H.T. Hewitt, C. Xiao, G. Aðalgeirsdóttir, S.S. Drijfhout, T.L. Edwards, N.R. Golledge, M. Hemer, R.E. Kopp, G. Krinner, A. Mix, D. Notz, S. Nowicki, I.S. Nurhati, L. Ruiz, J.-B. Sallée, A.B.A. Slangen, and Y. Yu, 2021: Ocean, Cryosphere and Sea Level Change. In Climate Change 2021: The Physical Science Basis. Contribution of Working Group I to the Sixth Assessment Report of the Intergovernmental Panel on Climate Change [Masson-Delmotte, V., P. Zhai, A. Pirani, S.L. Connors, C. Péan, S. Berger, N. Caud, Y. Chen, L. Goldfarb, M.I. Gomis, M. Huang, K. Leitzell, E. Lonnoy, J.B.R. Matthews, T.K. Maycock, T. Waterfield, O. Yelekçi, R. Yu, and B. Zhou (eds.)]. Cambridge University Press, Cambridge, United Kingdom and New York, NY, USA, pp. 1211–1362, doi:10.1017/9781009157896.011.

Garner, G.G., T. Hermans, R.E. Kopp, A.B.A. Slangen, T.L. Edwards, A. Levermann, S. Nowikci, M.D. Palmer, C. Smith, B. Fox-Kemper, H.T. Hewitt, C. Xiao, G. Aðalgeirsdóttir, S.S. Drijfhout, T.L. Edwards, N.R. Golledge, M. Hemer, G. Krinner, A. Mix, D. Notz, S. Nowicki, I.S. Nurhati, L. Ruiz, J.-B. Sallée, Y. Yu, L. Hua, T. Palmer, B. Pearson, 2021. IPCC AR6 Sea Level Projections. Version 20210809. https://doi.org/10.5281/zenodo.5914709.

Helmrich, A.M., Ruddell, B.L., Bessem, K., Chester, M.V., Chohan, N., Doerry, E., Eppinger, J., Garcia, M., Goodall, J.L., Lowry, C., Zahura, F.T., 2021. Opportunities for crowdsourcing in urban flood monitoring. Environ. Model. Softw. 143, 105124. https://doi.org/10.1016/j.envsoft.2021.105124.

Hendry, A., Haigh, I.D., Nicholls, R.J., Winter, H., Neal, R., Wahl, T., Joly-Laugel, A., Darby, S.E., 2019. Assessing the characteristics and drivers of compound flooding events around the UK coast. Hydrol. Earth Syst. Sci. 23, 3117–3139. https://doi.org/10.5194/hess-23-3117-2019.

Hino, M., Belanger, S.T., Field, C.B., Davies, A.R., Mach, K.J., 2019. High-tide flooding disrupts local economic activity. Sci. Adv. 5, eaau2736. https://doi.org/10.1126/sciadv.aau2736.

Hunter, N.M., Bates, P.D., Neelz, S., Pender, G., Villanueva, I., Wright, N.G., Liang, D., Falconer, R.A., Lin, B., Waller, S., Crossley, A.J., Mason, D.C., 2008. Benchmarking 2D hydraulic models for urban flooding. Proc. Inst. Civ. Eng. - Water Manag. 161, 13–30. https://doi.org/10.1680/wama.2008.161.1.13.

IPCC, 2021. Climate change 2021: the physical science basis: summary for policymakers: working group I contribution to the sixth Assessment report of the Intergovernmental Panel on Climate Change. [Masson-Delmotte, V., P. Zhai, A. Pirani, S.L. Connors, C. Péan, S. Berger, N. Caud, Y. Chen, L. Goldfarb, M.I. Gomis, M. Huang, K. Leitzell, E. Lonnoy, J.B.R. Matthews, T.K. Maycock, T. Waterfield, O. Yelekçi, R. Yu, and B. Zhou (eds.)]. Cambridge University Press, Cambridge, United Kingdom and New York, NY, USA.

Jacobs, J.M., Cattaneo, L.R., Sweet, W., Mansfield, T., 2018. Recent and Future Outlooks for Nuisance Flooding Impacts on Roadways on the U.S. East Coast. Transp. Res. Rec. 2672, 1–10. https://doi.org/10.1177/0361198118756366.

Kao, S.-C., DeNeale, S.T., Yegorova, E., Kanney, J., Carr, M.L., 2020. Variability of precipitation areal reduction factors in the conterminous United States. J. Hydrol. X 9, 100064. https://doi.org/10.1016/j.hydroa.2020.100064.

Karamouz, M., Zahmatkesh, Z., Goharian, E., Nazif, S., 2015. Combined impact of inland and coastal floods: mapping knowledge base for development of planning strategies. J. Water Resour. Plann. Manag. 141, 04014098. https://doi.org/10.1061/(ASCE)WR.1943-5452.0000497.

Karegar, M.A., Dixon, T.H., Malservisi, R., Kusche, J., Engelhart, S.E., 2017. Nuisance Flooding and Relative Sea-Level Rise: the Importance of Present-Day Land Motion. Sci. Rep. 7, 11197. https://doi.org/10.1038/s41598-017-11544-y.

Kew, S.F., Selten, F.M., Lenderink, G., Hazeleger, W., 2013. The simultaneous occurrence of surge and discharge extremes for the Rhine delta. Nat. Hazards Earth Syst. Sci. 13, 2017–2029. https://doi.org/10.5194/nhess-13-2017-2013.

Kim, J., Lee, J., Kim, D., Kang, B., 2019. The role of rainfall spatial variability in estimating areal reduction factors. J. Hydrol. 568, 416–426. https://doi.org/10.1016/j.jhydrol.2018.11.014.

Konrad, C.P., 2003. Effects of Urban Development on Floods, US Geological Survey Fact Sheet FS-076-03. Available from: ⟨https://pubs.usgs.gov/fs/fs07603/pdf/fs07603.pdf⟩ [Accessed June 7th, 2024].

Kopp, R.E., 2013. Does the mid-Atlantic United States sea-level acceleration hot spot reflect ocean dynamic variability? Geophys. Res. Lett. 40, 3981–3985. https://doi.org/10.1002/GRL.50781.

Kopp, R.E., Garner, G.G., Hermans, T.H.J., Jha, S., Kumar, P., Reedy, A., Slangen, A.B.A., Turilli, M., Edwards, T.L., Gregory, J.M., Koubbe, G., Levermann, A., Merzky, A., Nowicki, S., Palmer, M.D., Smith, C., 2023. The Framework for Assessing Changes to Sea-Level (FACTS) v1.0: A platform for characterizing

parametric and structural uncertainty in future global, relative, and extreme sea-level change. Geosci. Model Dev. 16, 7461–7489. https://doi.org/10.5194/gmd-16-7461-2023.
Kundzewicz, Z.W., Kanae, S., Seneviratne, S.I., Handmer, J., Nicholls, N., Peduzzi, P., Mechler, R., Bouwer, L.M., Arnell, N., Mach, K., Muir-Wood, R., Brakenridge, G. R., Kron, W., Benito, G., Honda, Y., Takahashi, K., Sherstyukov, B., 2014. Flood risk and climate change: global and regional perspectives. Hydrol. Sci. J. 59, 1–28. https://doi.org/10.1080/02626667.2013.857411.
Leandro, J., Chen, A.S., Djordjević, S., Savić, D.A., 2009. Comparison of 1D/1D and 1D/2D Coupled (Sewer/Surface) Hydraulic Models for Urban Flood Simulation. J. Hydraul. Eng. 135, 495–504. https://doi.org/10.1061/(ASCE)HY.1943-7900.0000037.
Lee, S.H., Kang, D.H., Byung Sik, B.S., 2018. A Study on the Method of Calculating the Threshold Rainfall for Rainfall Impact Forecasting. J. Korean Soc. Hazard Mitig. 18, 93–102. https://doi.org/10.9798/KOSHAM.2018.18.7.93.
Lendering, K.T., Jonkman, S.N., Kok, M., 2016. Effectiveness of emergency measures for flood prevention: Effectiveness of emergency measures. J. Flood Risk Manag. 9, 320–334. https://doi.org/10.1111/jfr3.12185.
Leopold, L.B., 1968. Hydrology for urban land planning: A guidebook on the hydrologic effects of urban land use. US Geological Survey.
Lian, J.J., Xu, K., Ma, C., 2013. Joint impact of rainfall and tidal level on flood risk in a coastal city with a complex river network: a case study of Fuzhou City, China. Hydrol. Earth Syst. Sci. 17, 679–689. https://doi.org/10.5194/hess-17-679-2013.
McCuen, R.H., 1998. Hydrologic Analysis and Design. Prentice Hall, New Jersey.
Merkel, W.H., Moody, H.F., Quan, Q.D., 2015. Design Rainfall Distributions Based on NOAA Atlas 14 Rainfall Depths and Durations. USDA NRCS Technical Paper.
Miro, M.E., DeGaetano, A., López-Cantú, T., Samaras, C., Webber, M., Grocholski, K.R., 2021. Developing Future Projected Intensity-Duration-Frequency (IDF) Curves: A Technical Report on Data, Methods, and IDF Curves for the Chesapeake Bay Watershed and Virginia. RAND Corporation. https://doi.org/10.7249/TLA1365-1.
Moftakhari, H.R., AghaKouchak, A., Sanders, B.F., Feldman, D.L., Sweet, W., Matthew, R.A., Luke, A., 2015. Increased nuisance flooding along the coasts of the United States due to sea level rise: Past and future. Geophys. Res. Lett. 42, 9846–9852. https://doi.org/10.1002/2015GL066072.
Moftakhari, H.R., AghaKouchak, A., Sanders, B.F., Matthew, R.A., 2017. Cumulative hazard: The case of nuisance flooding. Earth'S. Future 5, 214–223. https://doi.org/10.1002/2016EF000494.
Moftakhari, H.R., AghaKouchak, A., Sanders, B.F., Allaire, M., Matthew, R.A., 2018. What Is Nuisance Flooding? Defining and Monitoring an Emerging Challenge. Water Resour. Res. 54, 4218–4227. https://doi.org/10.1029/2018WR022828.
Morsy, M.M., Shen, Y., Sadler, J.M., Chen, A.B., Zahura, F.T., Goodall, J.L., 2019. Incorporating Potential Climate Change Impacts in Bridge and Culvert Design. Virginia Transportation Research Council Report VTRC 20-R13. Available from: ⟨https://vtrc.virginia.gov/media/vtrc/vtrc-pdf/vtrc-pdf/20-R13.pdf⟩ [Accessed June 7th, 2024].
NASA, 2021. Sea Level Projection Tool – NASA Sea Level Change Portal [Internet]. Available from: ⟨https://sealevel.nasa.gov/ipcc-ar6-sea-level-projection-tool⟩ [Accessed June 7th, 2024].
NRCS, 2019. Storm Rainfall Depth and Distribution. Part 630, Chapter 4 (210-NEH-630-4). NRCS Title 210. National Engineering Handbook, Washington, DC.
NRCS, 2022. WinTR–20 computer program for project formulation hydrology. Version 3.30.1. Washington, DC.
Pavlovic, S., Perica, S., St Laurent, M., Mejía, A., 2016. Intercomparison of selected fixed-area areal reduction factor methods. J. Hydrol. 537, 419–430. https://doi.org/10.1016/j.jhydrol.2016.03.027.
Praharaj, S., Zahura, F.T., Chen, T.D., Shen, Y., Zeng, L., Goodall, J.L., 2021. Assessing Trustworthiness of Crowdsourced Flood Incident Reports Using Waze Data: A Norfolk, Virginia Case Study. Transp. Res. Rec.: J. Transp. Res. Board 2675, 650–662. https://doi.org/10.1177/03611981211031212.
Ryan, P., Syme, B., Gao, S., Collecutt, G., 2022. Direct rainfall hydraulic model validation. Hydrology and Water Resources Symposium. Available from: ⟨https://www.tuflow.com/media/7545/2022-direct-rainfall-hydraulic-model-validation-ryan-et-al-hwrs.pdf⟩.
Shen, Y., Morsy, M.M., Huxley, C., Tahvildari, N., Goodall, J.L., 2019. Flood risk assessment and increased resilience for coastal urban watersheds under the combined impact of storm tide and heavy rainfall. J. Hydrol. 579, 124159. https://doi.org/10.1016/j.jhydrol.2019.124159.
Shen, Y., Tahvildari, N., Morsy, M.M., Huxley, C., Chen, T.D., Goodall, J.L., 2022. Dynamic Modeling of Inland Flooding and Storm Surge on Coastal Cities under Climate Change Scenarios: Transportation Infrastructure Impacts in Norfolk, Virginia USA as a Case Study. Geosciences 12, 224. https://doi.org/10.3390/geosciences12060224.
Silverman, A.I., Brain, T., Branco, B., Challagonda, P.S.V., Choi, P., Fischman, R., Graziano, K., Hénaff, E., Mydlarz, C., Rothman, P., Toledo-Crow, R., 2022. Making waves: Uses of real-time, hyperlocal flood sensor data for emergency management, resiliency planning, and flood impact mitigation. Water Res. 220, 118648. https://doi.org/10.1016/j.watres.2022.118648.
Skougaard Kaspersen, P., Høegh Ravn, N., Arnbjerg-Nielsen, K., Madsen, H., Drews, M., 2017. Comparison of the impacts of urban development and climate change on exposing European cities to pluvial flooding. Hydrol. Earth Syst. Sci. 21, 4131–4147. https://doi.org/10.5194/hess-21-4131-2017.
Sridhar, V., Modi, P., Billah, M.M., Valayamkunnath, P., Goodall, J.L., 2019. Precipitation Extremes and Flood Frequency in a Changing Climate in Southeastern Virginia. J. Am. Water Resour. Assoc. 55, 780–799. https://doi.org/10.1111/1752-1688.12752.
Svensson, C., Jones, D.A., 2010. Review of methods for deriving areal reduction factors. J. Flood Risk Manag. 3, 232–245. https://doi.org/10.1111/j.1753-318X.2010.01075.x.
Sweet, W., Park, J., Marra, J., Zervas, C., Gill, S., 2014. Sea Level Rise and Nuisance Flood Frequency Changes around the United States. NOAA Tech. Rep. NOS CO-OPS 073.
Sweet, W., Dusek, G., Obeysekera, J., Marra, J.J., 2018. Patterns and Projections of High Tide Flooding Along the U.S. Coastline Using a Common Impact Threshold. NOAA Tech. Rep. NOS CO-OPS 086.
Sweet, W.V., Marra, J.J., 2016. 2015 State of U.S. "Nuisance" Tidal Flooding. Available from: ⟨https://www.ncdc.noaa.gov/monitoring-content/sotc/national/2016/may/sweet-marra-nuisance-flooding-2015.pdf⟩ [Accessed June 7th, 2024].
Sweet, W.V., Hamlington, B.D., Kopp, R.E., Weaver, C.P., Barnard, P.L., Bekaert, D., Brooks, W., Craghan, M., Dusek, G., Frederikse, T., Garner, G., Genz, A.S., Krasting, J.P., Larour, E., Marcy, D., Marra, J.J., Obeysekera, J., Osler, M., Pendleton, M., Roman, D., Schmied, L., Veatch, W., White, K.D., Zuzak, C., 2022. Global and Regional Sea Level Rise Scenarios for the United States: Updated Mean Projections and Extreme Water Level Probabilities Along U. S. Coast. NOAA Tech. Rep. NOS 01.
Syme, W.J., 2001. TUFLOW – Two & one-dimensional Unsteady FLOW Software for Rivers, Estuaries and Coastal Waters. Pap. Present. IEAust Water Panel Semin. Workshop 2D Flood Model. Syd.
Taylor, M., Fisher, T., Pennington, M., Ng, K., Jackson, M. 2015. Increased Flooding Vulnerability - The Methodology and Flood Models to Assess 120,000 Properties in Christchurch. 2015 Asia Pacific Stormwater Conference. Available from: ⟨https://www.waternz.org.nz/Attachment?Action=Download&Attachment_id= 667⟩ [Accessed June 7th, 2024].
The City of Norfolk, 2018. A Green Infrastructure Plan for Norfolk. The City of Norfolk.
Wahl, T., Jain, S., Bender, J., Meyers, S.D., Luther, M.E., 2015. Increasing risk of compound flooding from storm surge and rainfall for major US cities. Nat. Clim. Change 5, 1093–1097. https://doi.org/10.1038/nclimate2736.
Wang, Y., Shen, Y., Salahshour, B., Cetin, M., Iftekharuddin, K., Tahvildari, N., Huang, G., Harris, D.K., Ampofo, K., Goodall, J.L., 2024. Urban flood extent segmentation and evaluation from real-world surveillance camera images using deep convolutional neural network. Environ. Model. Softw. 173, 105939. https://doi.org/10.1016/j.envsoft.2023.105939.
Woodruff, J.D., Irish, J.L., Camargo, S.J., 2013. Coastal flooding by tropical cyclones and sea-level rise. Nature 504, 44–52. https://doi.org/10.1038/nature12855.

Yin, J., Yu, D., Yin, Z., Liu, M., He, Q., 2016. Evaluating the impact and risk of pluvial flash flood on intra-urban road network: A case study in the city center of Shanghai, China. J. Hydrol. 537, 138–145. https://doi.org/10.1016/j.jhydrol.2016.03.037.
Zhang, T., Feng, P., Maksimović, Č., Bates, P.D., 2016. Application of a Three-Dimensional Unstructured-Mesh Finite-Element Flooding Model and Comparison with Two-Dimensional Approaches. Water Resour. Manag. 30, 823–841. https://doi.org/10.1007/s11269-015-1193-6.
Zhu, J., Stone, M.C., Forsee, W., 2012. Analysis of potential impacts of climate change on intensity–duration–frequency (IDF) relationships for six regions in the United States. J. Water Clim. Change 3, 185–196. https://doi.org/10.2166/wcc.2012.045.